JBIC (1999) 4:56–63

ORIGINAL ARTICLE

Annette Rompel · Helmut Fischer · Dirk Meiwes
Klaudia Büldt-Karentzopoulos · Renée Dillinger
Felix Tuczek · Herbert Witzel · Bernt Krebs

Purification and spectroscopic studies on catechol oxidases from *Lycopus europaeus* and *Populus nigra:* Evidence for a dinuclear copper center of type 3 and spectroscopic similarities to tyrosinase and hemocyanin

Received: 30 July 1998 / Accepted: 26 October 1998

Abstract We purified two catechol oxidases from *Lycopus europaeus* and *Populus nigra* which only catalyze the oxidation of catechols to quinones without hydroxylating tyrosine. The molecular mass of the *Lycopus* enzyme was determined to 39800 Da and the mass of the *Populus* enzyme was determined to 56050 Da. Both catechol oxidases are inhibited by thiourea, *N*-phenylthiourea, dithiocarbamate, and cyanide, but show different pH behavior using catechol as substrate. Atomic absorption spectroscopic analysis found 1.5 copper atoms per protein molecule. Using EPR spectroscopy we determined 1.8 Cu per molecule catechol oxidase. Furthermore, EPR spectroscopy demonstrated that catechol oxidase is a copper enzyme of type 3. The lack of an EPR signal is due to strong antiferromagnetic coupling that requires a bridging ligand between the two copper ions in the *met* preparation. Addition of H_2O_2 to both enzymes leads to *oxy* catechol oxidase. In the UV/Vis spectrum two new absorption bands occur at 345 nm and 580 nm. In accordance with the *oxy* forms of hemocyanin and tyrosinase the absorption band at 345 nm is due to an O_2^{2-} $(\pi_\sigma^*) \rightarrow$ Cu(II) $(d_{x^2-y^2})$ charge transfer (CT) transition. The absorption band at 580 nm corresponds to the second O_2^{2-} $(\pi_v^*) \rightarrow$ Cu(II) $(d_{x^2-y^2})$ CT transition. The UV/Vis bands in combination with the resonance Raman spectra of *oxy* catechol oxidase indicate a μ-η^2:η^2 binding mode for dioxygen. The intense resonance Raman peak at 277 cm^{-1}, belonging to a Cu-N (axial His) stretching mode, suggests that catechol oxidase has six terminal His ligands, as known for molluscan and arthropodan hemocyanin.

Key words Metalloprotein · Type 3 copper center · Tyrosinase · Hemocyanin · Oxygen binding

Abbreviations *CT* charge transfer · *MALDI-MS* matrix-assisted laser desorption/ionization mass spectrometry

Introduction

The two prominent members among the copper proteins with a type 3 center in the active site are hemocyanin and tyrosinase (see [1–5] and references therein). Hemocyanin is an oligomeric oxygen transport protein of molluscs and arthropods. It binds oxygen at a dinuclear active site containing two copper atoms directly bound by protein side chains. The protein was first isolated and crystallized by Kubowitz [6]. In recent years, advances have been reported in determining the crystal structures of two arthropodan hemocyanins from *Panulirus interruptus* [7] and *Limulus polyphemus,* the latter in its deoxygenated [8] and oxygenated [9] forms. Recently, a structure of molluscan hemocyanin has been published [10].

The active site of *deoxy* hemocyanin from the arthropod *Panulirus interruptus* [7, 11] contains two Cu(I) atoms 3.5 Å apart. For *deoxy Limulus polyphemus* hemocyanin the Cu-Cu distance is 4.6 ± 0.2 Å. Each Cu(I) is coordinated by three histidines, two of them tightly bound (Cu-N $<$ 2.0 Å) and a third one at a longer distance (Cu-N $\sim$ 2.7 Å). There is no bridge present to link both Cu atoms.

The addition of O_2 generates *oxy* hemocyanin. While the crystal structure of *oxy Panulirus interruptus*

A. Rompel · K. Büldt-Karentzopoulos · B. Krebs (✉)
Anorganisch-Chemisches Institut der Universität Münster,
Wilhelm-Klemm-Strasse 8, D-48149 Münster, Germany
e-mail: krebs@nwz.uni-muenster.de,
Tel.: +49-251-8333131, Fax: +49-251-8338366

A. Rompel · H. Fischer · D. Meiwes
K. Büldt-Karentzopoulos · H. Witzel
Institut für Biochemie der Universität Münster,
Wilhelm-Klemm-Strasse 2, D-48149 Münster, Germany

R. Dillinger · F. Tuczek
Institut für Anorganische Chemie und Analytische Chemie der Universität Mainz, Staudingerweg 9, D-55099 Mainz, Germany

H. Witzel died on 1 September 1996

Dedicated to Professor Wolfram Saenger on the occasion of his 60th birthday

hemocyanin is unknown, the copper copper distance is significantly shorter (3.6 ± 0.2 Å) in *oxy* than in *deoxy Limulus polyphemus* hemocyanin. Before the crystal structure was available, Cu-Cu distances of about 3.6 Å were obtained from extended X-ray absorption fine structure (EXAFS) data [12–15]. X-ray structure analysis revealed that upon oxidation the coordinated histidines move very little [9]. The oxygen is bound in the μ-η^2:η^2 mode [16, 17] first reported by Kitajima et al. [18] for a synthetic dinuclear copper model complex. Apart from the protein absorption feature at 280 nm, a relatively strong absorption in the range of 335–350 nm ($\varepsilon = 20000\ M^{-1}\ cm^{-1}$) is observed in *oxy* hemocyanin which is assigned to a peroxo O_2^{2-} (π_σ^*)→Cu(II) ($d_{x^2-y^2}$) charge transfer (CT) transition [4, 5, 19, 20]. Another absorption band is seen around 580 nm ($\varepsilon = 1000\ M^{-1}\ cm^{-1}$). It is assigned to a peroxo O_2^{2-} (π_v^*)→Cu(II) ($d_{x^2-y^2}$) CT transition [4, 5, 19, 20].

Tyrosinase (monophenol, *o*-diphenol: oxygen oxidoreductase, EC 1.14.18.1) is a copper enzyme that is widely distributed throughout microorganisms, plants, and animals. It is of central importance in such processes as vertebrate pigmentation and the browning of fruits and vegetables [21]. The active site contains a dinuclear copper center of type 3. The enzyme catalyzes two different reaction types: (1) the *ortho*-hydroxylation of monophenols (monophenolase activity) and (2) the oxidation of *o*-diphenols to *o*-quinones (diphenolase activity), both reactions with electron transfer to oxygen. Tyrosinase is present in three states: *met, deoxy,* and *oxy* [22–24]. An X-ray structure analysis is not available for any state of tyrosinase.

EXAFS studies [25] of *Neurospora crassa* tyrosinase revealed a Cu(II)-Cu(II) distance of 3.6 Å for the *oxy* species and 3.4 Å for the *met* form. For both the first shell is reported to consist of two nitrogen ligands at a distance of 2.0 Å and two or three oxygen ligands at a distance of 1.9 Å. In contrast to hemocyanin, with identical sets of ligands, it is probable that both Cu(II) ions are not surrounded by an identical set of ligands; differences in their geometry should be expected. Evidence for an asymmetric ligand environment has been obtained from the kinetics of the apoenzyme reconstitution with Cu(II) [26].

In analogy to hemocyanin, the enzyme shows a CT band at 345 nm after addition of H_2O_2 as well as a weak absorption band at 590 nm [20, 24]. The resonance Raman spectrum of the *oxy* form shows a band at 755 cm^{-1} characteristic for a μ-η^2:η^2 binding mode for dioxygen [27].

The complexity of the tyrosinase reaction suggests looking for other enzymes catalyzing exclusively the catechol oxidation to quinone, but not a hydroxylation reaction as tyrosinase does. In this paper we report on two monomeric catechol oxidases from *Populus nigra,* first described by Trémolière and Bieth [28], and from *Lycopus europaeus* [29], which convert caffeic acid to quinones and furthermore to melanines at injured cells.

Materials and methods

Preparation of catechol oxidases

All operations were performed at 4 °C. The catechol oxidases were isolated according to modified procedures described by Trémolière and Bieth [28] for the *Populus* enzyme and by Fischer for the *Lycopus* enzyme [29]. The leaves were washed 2–3 times with double-distilled water before lyophilization. A typical preparation started with 40 g lyophilized leaves which were suspended in 1.4 l buffer (0.05 M imidazole, 0.1 M sodium ascorbate, 0.3% Triton X-100; pH 6.0). The leaves were broken and homogenized with an Ultra-Turrax (6000 rpm) in the presence of 60 g poly(vinylpyrrolidone) (PVP, Sigma), in order to absorb low molecular mass phenolic compounds like caffeic acid, the natural substrate. The homogenate was centrifuged at 10000 *g* for 1 h and the supernatant liquid filtered through glass wool. A 1.5-fold volume of ethanol was slowly added to the solution and stirred for another 2 h. After 30 min of centrifugation at 10000 *g* the precipitate was resuspended two times in 400 ml 0.05 M triethanolamine/acetic acid (pH 5.8) with 0.025 M sodium ascorbate under stirring for several hours. The solution was again centrifuged at 10000 *g*.

First ion-exchange chromatography

The supernatant was loaded onto a DEAE-cellulose column (Pharmacia, 30 cm × 2 cm) equilibrated with triethanolamine/acetic acid (pH 5.8) at a flow rate of 40 ml/h. Catechol oxidase was passed through and the active fractions were pooled. The sample was equilibrated with 0.05 M triethanolamine acetate (pH 6.8) by dialysis.

Second ion-exchange chromatography

The active fractions were loaded on a Q = Sepharose FF (Pharmacia, 20 cm × 2 cm) and eluted with a 0–0.8 M NaCl gradient, flow rate 40 ml/h. Catechol oxidase was released from the column at a NaCl concentration of 0.5 M.

Gel filtration

The active fraction collected from Q-Sepharose FF was concentrated to 5 ml, equilibrated with 0.05 M sodium phosphate (pH 7), and then applied to a Sephadex G-75 superfine column (Pharmacia, 100 cm × 2 cm). The column was eluted with the same buffer at a flow rate of 0.5 ml/min. The active fractions were pooled and stored at 4 °C without loss of activity for several months.

Enzyme activity

The activity of the enzyme during the purification was monitored by spectrophotometric measurements of the oxidation products of catechol at 420 nm. Two different enzyme assays were performed. Catechol oxidase activity was measured toward 3 mM catechol. The reaction was performed at 20 °C in 1 ml of reaction mixture containing 0.1 M sodium phosphate buffer (pH 6.5), 3 mM catechol substrate, and suitable amounts of enzyme. One unit (U) of enzyme activity is defined as the amount of enzyme which increased the absorbance by 1 per min during the oxidation of 3 mM catechol at 20 °C [28].

To determine catechol oxidase activity in the presence of reducing agents – in order to prevent secondary reactions of the produced quinones – sodium ascorbate was added to the sample. The reaction mixture contains 0.1 M sodium phosphate buffer (pH 6.5), 1 mM sodium ascorbate, and 0.3 mM catechol. The reaction is initiated by the addition of sufficient enzyme to cause decrease of absorbance at 265 nm (ascorbate: $\varepsilon_{265} = 15300\ M^{-1}$

cm^{-1}) with 0.3 mM catechol. The decrease of absorbance at 265 nm is due to the formation of dehydroascorbate. One unit (U) of enzyme activity is defined as the amount of enzyme which decreases the absorbance by 0.1 per min. For both enzyme assays the change in absorption was recorded for about 5 min and initial rates were calculated by drawing tangents to the initial part of the kinetic curves.

Protein content

Protein concentration was determined both by the method of Bradford [30], with bovine serum albumin (BSA) as a standard, and by measuring the absorbance at 280 nm.

M_r measurements

The molecular mass of catechol oxidase was determined by SDS-PAGE. The following marker proteins (Pharmacia) were used: phosphorylase b (94000 Da), BSA (67000 Da), ovalbumin (43000 Da), carbonic anhydrase (30000 Da), trypsin inhibitor (20100 Da), and α-lactalbumin (14400 Da). SDS-PAGE for molecular mass determination was done for both enzymes on SDS/10% (w/v) polyacrylamide gels. SDS-PAGE was stained with Coomassie brilliant blue R 250.

Matrix-assisted laser desorption/ionization mass spectrometry (MALDI-MS) was performed on a reflectron-type time-of-flight mass spectrometer (Lamma 1000, Leybold Heraeus). The apparatus is described in detail elsewhere [31, 32]. In this study a nitrogen laser (Laser Science) with an emission wavelength of 337 nm and 3-ns pulse duration was used. The concentrations of the analyzed compounds were between 1 μM and 10 μM in double-distilled water. The analyte solutions were mixed in a ratio of 1:10 with the matrix solutions. Up to 1 μl of this mixture (containing 0.1–1 pmol) was gently dried on an inert metal surface before introduction into the mass spectrometer.

The matrix solution consists of 2,5-dihydroxybenzoic acid at a concentration of 10 g/l in 10% ethanol. For calibration of the mass spectra a mixture of insulin (bovine), cytochrome *c* (horse), and myoglobin (horse) was used as external standard. Mass accuracy was in the range 0.001–0.005% [31]. The spectra refer to an average of 10 scans.

pH dependence

The pH-rate profiles were measured using the catechol test and the catechol/ascorbate test over the pH range 4–10.5. Two buffer systems were used. One consisted of 0.05 M piperazine/0.05 M triethanolamine. This mixture was titrated with HCl or NaOH to give buffers over the pH range 4.5–10.5. Alternatively, the following buffers were used: (1) 0.1 M sodium phosphate, pH 4.0–8.0; (2) glycine/NaOH, pH 8.0–10.0. The activity assay for the pH profile was performed as described above. Measurements of activity were made in duplicate at each pH. No enzyme denaturation or non-enzymatic oxidation of catechol occurred in this mixed buffer systems at any pH used.

Inhibitors

N-Phenylthiourea, thiourea, sodium *N,N*-diethyldithiocarbamate, potassium cyanide, and 1,10-phenanthroline were purchased from Sigma and used as received. Catechol oxidase (8 μg) was incubated with 1 mM inhibitor in 0.01 M sodium phosphate buffer (pH 6.8) for several hours at 4 °C. Afterwards the mixture was brought to 25 °C and the reaction was initiated by the addition of catechol. Measurements of activity were made in duplicate for each inhibitor.

Atomic absorption spectroscopy

Cu, Fe, and Zn were determined by graphite furnace absorption spectroscopy. Appropriate controls of the buffer solutions used to purify these enzymes were analyzed and their metal content subtracted.

EPR measurements

EPR spectra were performed at the Institute for Physical Chemistry, University of Münster, using a Bruker ESP 300 spectrometer equipped with a TE_{102} resonator. Spectra were recorded at 77 K with a microwave frequency of 9.37 GHz and a modulation frequency of 100 kHz. The enzyme concentration was 3.4×10^{-4} M in 200 μl of 0.05 M triethanolamine/acetic acid (pH 7.0). Denaturation was achieved by addition of 200 μl 6 M HNO_3. This dilution of the enzyme by a factor of two has been taken into account for the determination of copper. The solution was frozen in liquid nitrogen. For the quantification of Cu^{2+}, $CuSO_4 \cdot 5H_2O$ standard solutions containing Cu^{2+} in the range between 5.0×10^{-5} mol/l and 5.0×10^{-4} mol/l have been prepared and their EPR spectra recorded.

UV/Vis spectroscopic studies

Visible and UV spectra of the enzymes were recorded at 20 °C in 50 mM sodium phosphate buffer (pH 7.0) in a 1 cm quartz cuvette with a Shimadzu UV 2100 spectrophotometer.

Resonance Raman

UV resonance Raman spectra of *oxy* catechol oxidase were recorded on a home-built spectrometer at the University of Mainz consisting of a SPEX 1404 0.85 m double monochromator equipped with a nitrogen-cooled CCD camera (PI Instruments, 1024×256 EEV chip, spectral coverage: 1000 cm^{-1} @ 350 nm). Excitation source was a Spectra Physics 2080 Kr^+ laser (350.7 nm). Typically spectra were run with laser powers around 20 mW and acquisition times of 100 s. Spectra were obtained on 5×10^{-4} M solutions at room temperature and on frozen solutions at 100 K using a liquid helium cryostat (CryoVac). The Raman-active *oxy* form was generated by addition of saturating amounts of H_2O_2 to the *met* form. After taking 4–5 spectra, it was necessary to regenerate the *oxy* form by adding H_2O_2. The final spectrum was obtained by summation of nine 100 s spectra.

Results

Purification and reactivity of catechol oxidase

Purification

The purification procedure for the *Lycopus* catechol oxidase is summarized in Table 1. The numbers reported are an average of five purification procedures. We obtained a nearly identical scheme for the *Populus* enzyme. The first steps of the purification scheme, through PVP and DEAE-cellulose, were performed to eliminate the phenolics that are present in the plant cells. Additionally, pigments remain adsorbed on the top of the DEAE-cellulose column. The eluent contains the catechol oxidase together with a peroxidase and some other components. The peroxidase, also observed by Trémolière and Bieth [28], is obviously a

Table 1 Purification of catechol oxidase from *Lycopus europaeus*

Step	Total activity (units)	Total protein (mg)	Specific activity (units/mg)	Purification (fold)	Yield (%)
Solubilized pellet of ethanol precipitation	4470	1490	3	1	100
DEAE-cellulose	3750	420	9	3	84
Q-Sepharose	3310	33	100	33	74
Sephadex G-75	3080	10	308	100	69

heme protein because of its absorption band at 405 nm. It can be separated from the catechol oxidase by the subsequent Q-Sepharose column. If necessary, this procedure can be repeated in order to obtain a peroxidase-free catechol oxidase. Trémolière and Bieth [28] copurified catechol oxidase with a peroxidase. In this paper we show that peroxidase can be seperated from catechol oxidase by a Q-Sepharose column. Other contaminants could be separated with a Sephadex G-75 column from catechol oxidase, which in the SDS-PAGE shows one band after staining with Coomassie brilliant blue R 250. Moreover, MALDI-MS did not yield other contaminant signals. Both catechol oxidases are stable in 0.05 M sodium phosphate buffer at pH 7.0 for months in the refrigerator at 4 °C.

Enzyme reaction

The action of the enzymes on their natural substrate caffeic acid and the following non-enzymatic steps for the formation of melanines have been reported in detail elsewhere [29]. Figure 1 shows the reaction of catechol oxidase from *Lycopus* with low concentrations of catechol. It first leads to the *o*-benzoquinone with an absorption at 390 nm. After 1 h the main products are the dimeric intermediates with λ_{max} at 410 nm first described by Forsyth et al. [33, 34] and finally the sample becomes dark-brown by melanine production. With caffeic acid, obviously the natural substrate, we obtain several intermediates. The products are documented in [29] and correspond to those obtained after a non-enzymatic oxidation of caffeic acid by $KMnO_4$ [35, 36].

Molecular mass

The molecular mass (M_r) calculated by SDS electrophoresis was 40 kDa for the *Lycopus* enzyme and 55 kDa for the *Populus* enzyme. Figure 2 shows the MALDI spectrum of catechol oxidases from *Lycopus* (2A) and *Populus* (2B). Singly charged molecules with M_r of 39800 for the *Lycopus* monomer (M^+) are detected as well as the multiply charged molecules M^{2+} and M^{3+} with signals around 20000 and 14000 Da, respectively. For the *Populus* enzyme a M_r of 56050 Da is found, nearly the same as reported before [28]. The multiply charged monomeric molecules at 28000 and 18700 Da are also seen.

pH dependence

The nature of ionizable groups affecting enzyme activity can be determined by examining the pH dependence of v_{max}. A plot of v_{max} versus pH of the *Lycopus* en-

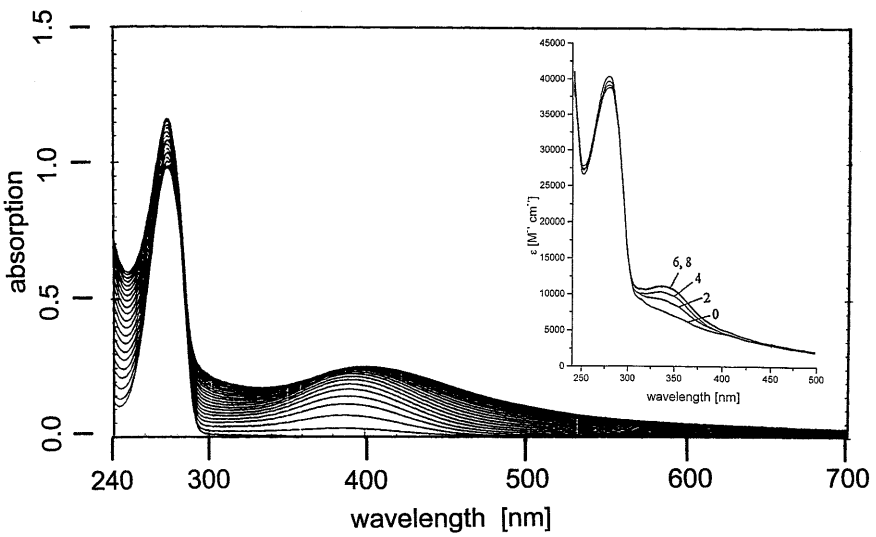

Fig. 1 UV/Vis spectra of catechol oxidase from *Lycopus europaeus* with low concentrations of catechol. Scans were taken every 3 min. *Inset:* UV/Vis absorption spectrum of catechol oxidase from *Lycopus* in 0.05 M sodium phosphate (pH 7), before and after addition of 2, 4, 6, and 8 equiv of H_2O_2

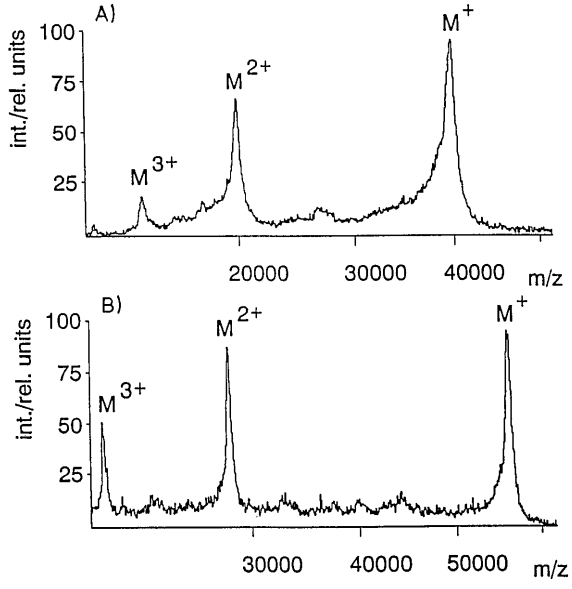

Fig. 2A, B Matrix-assisted laser desorption/ionization mass spectra of native *Lycopus* (**A**) and *Populus* (**B**) catechol oxidase

zyme using catechol showed a parabolic dependence, with a maximum between pH 6.5 and 7.5. The pH rate profile indicates two essential residues with pK_a values of 6 and 9. The pK_a value of 6 is consistent with histidine, but other amino acids could give similar values depending on the local environment. In order to ensure that the data do not arise from artifacts, two different buffer systems were used at each pH value as described in the Materials and methods. We obtained the same pH dependence.

For the *Populus* enzyme the activity increases with increasing pH over the range 5.0–8.0 in a biphasic manner, with a plateau between pH 6 and 7.0. The optimum pH for activity is approximately 8.0, with activity decreasing at higher pH values. The biphasic pH dependence of catechol activity that we find for the *Populus* enzyme has been observed before [28] and is consistent with at least two deprotonated groups being involved in catalysis. For both enzymes, irreversible loss of activity occurs below pH 4.0 and above pH 10.0.

Inhibitors

Evidence for a copper enzyme can be obtained from specific inhibition reactions for both enzymes. The effect of inhibitors on both enzymes at pH 7.0 is quite similar. They are inhibited by *N*-phenylthiourea, thiourea, and sodium *N,N*-diethyldithiocarbamate, which also inhibit tyrosinase and hemocyanin [37]. In addition, both catechol oxidases are blocked completely by cyanide. 1,10-Phenanthroline showed little effect on catechol oxidase activity. The same is known for tyrosinase, as described by Chakraborty et al. [38].

Analyses of metal centers

Atomic absorption spectroscopy

The metal content AAS analysis of purified catechol oxidase supports the hypothesis that copper is the metal bound in the active site of catechol oxidase. The purified preparation of catechol oxidase contains around 1.5 copper atoms per protein molecule, but no significant amounts of Fe and Zn have been observed. The value of 1.5 is low, owing to partial loss of Cu during purification and concentration of the protein sample (see also EPR measurements).

EPR measurements

Tyrosinase and hemocyanin are metalloproteins which contain an EPR-nondetectable dinuclear copper active site often classified as type 3 copper. To further characterize the metal center of catechol oxidase we recorded the EPR spectrum of *met Lycopus* catechol oxidase in 0.05 M triethanolamine/acetic acid, pH 7.0 (see Fig. 3; upper trace). A very weak Cu^{2+} EPR signal at $g=2$ was obtained. After addition of 6 M HNO_3, denaturation of the protein occurred and a typical cupric signal appears (lower trace). The EPR spectrum of the denatured sample is characteristic for Cu^{2+} in a tetragonal field. The intensive signal for $g_\perp$ appears at 323 mT ($g=2.073$) and the signal for $g_\parallel$ at 279 mT ($g=2.400$). A nearly identical EPR spectrum was obtained for the *Populus* enzyme.

We conclude that catechol oxidase contains a dinuclear cupric derivative which is EPR-nondetectable and belongs to the type 3 copper sites. The very weak Cu^{2+} EPR signal at $g=2$ seen for *met* catechol oxidase is due to a small fraction of sites that have become disrupted. A small EPR signal has been observed before in *met* preparations of hemocyanin and tyrosinase [39–41].

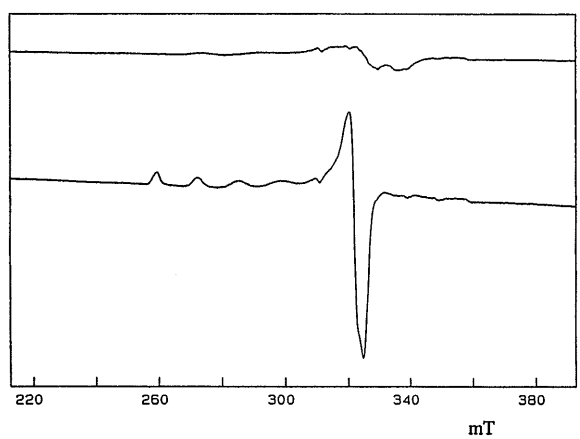

Fig. 3 X-band EPR spectra of native catechol oxidase of *Lycopus (upper trace)* and the same sample after denaturation with 6 M HNO_3 (*lower trace*)

This is due to a partial loss of copper during purification and concentration of the protein.

EPR spectroscopy has been used for the quantitation of cupric copper [42]. The number of copper atoms present in catechol oxidase can be determined by comparing the signal intensity of the fully denatured protein sample with $CuSO_4 \cdot 5H_2O$ standards in different concentrations. We found 1.8 mol Cu^{2+} per mol catechol oxidase. This result is further evidence for a dinuclear copper site and led us conclude that 10% of the dinuclear copper sites are disrupted in the concentrated *met* preparation. For both catechol oxidases, another EPR scan was taken over the range 50–450 mT. There is no signal in the 150 mT region, which excludes Fe(III) or a triplet state of dinuclear Cu(II).

UV/Vis spectroscopic studies

The electronic spectrum of *met* catechol oxidase from *Lycopus* in 0.05 M sodium phosphate (pH 7.0) after addition of H_2O_2 is presented in the inset of Fig. 1 (trace 6, 8). The *met* enzyme is also shown in the inset of Fig. 1 (trace 0). The maximum of the protein part is seen at 280 nm, indicating the presence of the amino acid tyrosine. For the *Lycopus* enzyme a weak shoulder and for the *Populus* enzyme an even less pronounced feature is observed at 288 nm, pointing toward low amounts of tryptophan. Additionally, both enzymes exhibit in their *met* form a shoulder around 330 nm, which has been observed before for tyrosinase [24]. The missing of an intense absorption band at 600 nm, which belongs to a cysteine sulfur to copper CT transition, excludes type 1 copper being present in the *met* form of both catechol oxidases [4, 5].

Addition of H_2O_2 to the *Lycopus* enzyme and the *Populus* enzyme leads to two new absorption bands at 345 nm and 580 nm (see inset of Fig. 1, trace 6). Saturation of the *Lycopus* band at 345 nm with an ε-value of $\sim 11\,000\ M^{-1}\ cm^{-1}$ per protein – erroneously reported before as $3500\ M^{-1}\ cm^{-1}$ [43] – is reached with 6 equiv of H_2O_2 (see inset of Fig. 1). For the *Populus* enzyme, 80 equiv are needed to saturate the band at 345 nm ($\varepsilon_{345} = 6000\ M^{-1}\ cm^{-1}$ per protein). A possible explanation is that the *oxy* form is more labile than the corresponding *oxy* form of the *Lycopus* enzyme. The appearence of these two absorption bands after addition of H_2O_2 has been reported for hemocyanin and tyrosinase [4, 5, 19, 20, 24]. According to Eickman et al. [19], the absorption band at 345 nm has to be attributed to the *oxy* form of the protein and is caused by an O_2^{2-} $(\pi_\sigma^*) \rightarrow$ Cu(II) $(d_{x^2-y^2})$ CT transition. The absorption band at 580 nm corresponds to the second O_2^{2-} $(\pi_v^*) \rightarrow$ Cu(II) $(d_{x^2-y^2})$ CT transition as found in *oxy* hemocyanin and *oxy* tyrosinase [4, 5, 19, 20, 24]. The values reported here for catechol oxidase are lower than those reported for hemocyanin and tyrosinase.

Additionally, higher concentrations of H_2O_2 lead to a time-dependent reaction with an isosbestic point and to inactivation, indicating decay of the peroxo complex. In oxygen-free solution, oxygen is produced with the disappearance of H_2O_2, indicating catalase activity as is also found for molluscan hemocyanin and tyrosinase [4, 44].

Resonance Raman

The Raman active *oxy* form of catechol oxidase from *P. nigra* proved to be extremely labile in the 350 nm laser beam. Nevertheless, using low laser powers, short irradiation times, multiple spectral acquisition, and addition of H_2O_2 between measurements, we were able to obtain UV resonance Raman spectra of this enzyme. The strongest peak is observed at 277 cm^{-1} (Fig. 4), in agreement with the UV resonance Raman spectrum of *oxy* tyrosinase [27] and *oxy* hemocyanin [45]. For *oxy* hemocyanin this band has been assigned to the Cu-N_{ax} (axial His) stretching mode [45]. Alternatively, an assignment to a symmetric Cu_2O_2 core stretch primarily involving copper motion has been suggested [46]. In any case, the observation of this mode proves the existence of a μ-η^2:η^2 peroxide-bridged structure at the dinuclear copper active site in catechol oxidase. Further

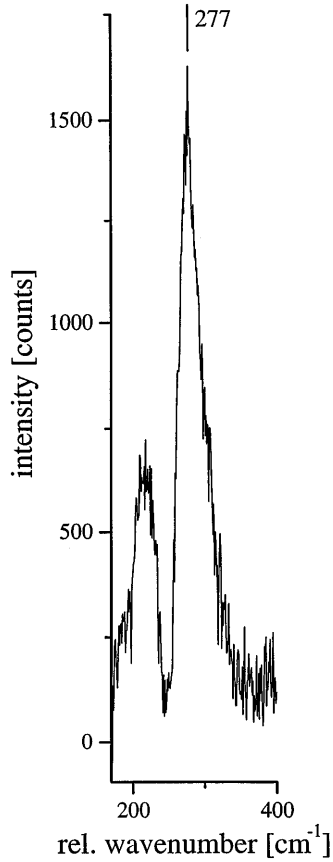

Fig. 4 UV resonance Raman spectrum of *oxy* catechol oxidase from *Populus* at room temperature; $\lambda_{exc} = 350.7$ nm, 20 mW, spectral resolution 14 cm^{-1}, 900 s

evaluation of the Raman spectrum is very difficult because of a steeply increasing background due to fluorescence. The resulting increase of signal noise almost completely obscures the Raman peaks at higher wavenumbers. In particular, it is difficult to identify the characteristic O-O stretching frequency of the μ-η^2:η^2 peroxide-bridged dinuclear copper unit around 750 cm^{-1} as is observed in the model complex [Cu{HB(3,5-$iPr_2pz)_3$}]$_2(O_2)$ [46, 47] and in *oxy* hemocyanin [45]. In catechol oxidases from sweet potatoes, however, the peroxide stretching vibration can be observed at this position besides the peak at $\sim$280 cm^{-1} (unpublished results).

Discussion

Catechol oxidases lack monophenol monooxygenase (cresolase) activity. The enzyme catalyzes only the oxidation of aromatic 1,2-diols to *o*-quinones. In subsequent reaction steps the primary products form dimers and finally oligomeric products known as melanines. Dioxygen, which is reduced to water, is the electron acceptor. In plants caffeic acid and its derivatives are the natural substrates, stored in the vacuole.

There are several reports about catechol oxidases in the literature, but so far all of them are poorly characterized. We previously reported initial characterization of two catechol oxidases from *L. europaeus* and *P. nigra* [43]. Here a spectroscopic characterization of both enzymes is reported.

The active site of catechol oxidase contains an antiferromagnetically coupled copper center of type 3, clearly evidenced by the EPR data in Fig. 3. Other type 3 copper proteins are hemocyanin, the oxygen transport protein of arthropods and molluscs, and tyrosinase, the enzyme that hydroxylates tyrosine to dopa and oxidizes dopa to dopa quinone. The latter reaction is chemically identical with the one catalyzed by catechol oxidase. All these type 3 copper proteins have in common the binding of dioxygen.

Met catechol oxidase contains two Cu(II) ions but exhibits no EPR signal, owing to strong antiferromagnetic coupling between the two $S=1/2$ metal ions. The antiferromagnetic coupling requires a superexchange pathway associated with a bridging ligand. In general, *met* preparations of catechol oxidase and tyrosinase as well as the decomposed peroxo complex exhibit a very weak absorption around 330 nm. One or two μ-hydroxo groups bridging the two Cu ions could explain these bands [48]. Further support for hydroxide bridging the two Cu(II) in the *met* form comes from EXAFS results reported before [43, 49]. The short Cu(II)-Cu(II) distance of 2.93 Å indicates one or two monoatomic bridges. In the complex [Cu{HB(3,5-$Me_2pz)_3$}]$_2(OH)_2$ containing two μ-hydroxo bridges, Kitajima and Moro-oka [50] reported a copper-copper distance of 2.93 Å, determined by crystal structure analysis, and a strong antiferromagnetic coupling. Addition of H_2O_2 to the complex leads to the μ-η^2:η^2 peroxo complex.

Oxy catechol oxidase can be obtained by adding oxygen to *deoxy* catechol oxidase or by addition of H_2O_2 to the Cu(II)-Cu(II) *met* catechol oxidase. Evidence for the oxygen binding mode can be derived from spectroscopic data of the *oxy* form. *Oxy* catechol oxidase shows two characteristic peroxo$\rightarrow$Cu(II) CT transitions. The absorption band at 345 nm is caused by an O_2^{2-} (π_σ^*)$\rightarrow$Cu(II) ($d_{x^2-y^2}$) CT transition. The absorption band at 580 nm corresponds to the second O_2^{2-} (π_v^*)$\rightarrow$Cu(II) ($d_{x^2-y^2}$) CT transition as found in *oxy* hemocyanin and *oxy* tyrosinase [4, 5, 19, 20, 24]. Both bands appear at the same position and for the *Lycopus* enzyme with the same intensity, as was reported for *oxy* hemocyanin and *oxy* tyrosinase. The fact that the CT bands of *oxy* catechol oxidase appear at the same position compared to hemocyanin and tyrosinase indicates a μ-η^2:η^2 binding mode for dioxygen and suggests that both copper atoms in catechol oxidase are coordinated by three nitrogen ligands from histidine, as is known from the X-ray structure of molluscan and arthropodan hemocyanin. Furthermore, the resemblance of the observed UV resonance Raman spectrum to those of *oxy* tyrosinase [27] and *oxy* hemocyanin [45] shows that the active sites are very similar in all three proteins. Based on the assignment of Ling et al. [45], the Raman peak at $\sim$277 cm^{-1} can be considered as a proof for an axial His ligand being also present in catechol oxidase. Unfortunately, it has not been possible to identify the characteristic O-O stretching vibration around 750 cm^{-1} in this enzyme. Owing to the thermal and photochemical lability of the *oxy* form and a large fluorescence background, the measurement of Raman spectra proved to be extremely difficult. Nevertheless, the combined evidence from UV/Vis (CT bands at 345 nm and 580 nm) and Raman spectroscopy (277 cm^{-1} peak) unequivocally shows that in *oxy* catechol oxidase a peroxide is bridging two copper centers in a μ-η^2:η^2 binding mode with each copper coordinated by three histidine ligands (two equatorial, one axial). To conclude, catechol oxidase has an active site that is closely related to that of the known type 3 copper proteins hemocyanin and tyrosinase.

Acknowledgements This paper is dedicated to the memory of the late Professor Herbert Witzel who was the spiritus rector of the early stages of this work. Financial support from the Deutsche Forschungsgemeinschaft under Kr 406/13-2 and Wi 124/26-4 and from the Fonds der Chemischen Industrie is gratefully acknowledged. We thank Annette Brümmer for her excellent technical assistance, Dr. B. Stahl, Institut für Medizinische Physik (Prof. F. Hillenkamp) for the MALDI-MS measurements and Dr. R. Bogumil for the EPR experiments. The paper is in partial fulfilment of the requirements for the degree of Dr. rer. nat. of D. M. and K. B.-K. at the Westfälische Wilhelms-Universität, Münster.

References

1. Malkin R, Malmström BG (1970) Adv Enzymol 33:177–244
2. Malmström BG (1982) Annu Rev Biochem 51:21–59
3. Solomon EI, Sundaram UM, Machonkin TE (1996) Chem Rev 96:2563–2605
4. Solomon EI, Baldwin MJ, Lowery MD (1992) Chem Rev 92:521–542
5. Solomon EI, Tuczek F, Root DE, Brown CA (1994) Chem Rev 94:827–856
6. Kubowitz F (1938) Biochem Z 299:32–57
7. Volbeda A, Hol WGJ (1989) J Mol Biol 209:249–279
8. Hazes B, Magnus KA, Bonaventura C, Bonaventura J, Dauter Z, Kalk KH, Hol WGJ (1993) Protein Sci 2:597–619
9. Magnus KA, Hazes B, Ton-That H, Bonaventura C, Bonaventura J, Hol WGJ (1994) Proteins 19:302–309
10. Cuff ME, Miller KI, Van Holde KE, Hendrickson WA (1998) J Mol Biol 278:855–870
11. Gaykema WPJ, Hol WGJ, Vereijken JM, Soeter NM, Bak HJ, Beintema JJ (1984) Nature 309:23–29
12. Co MS, Hodgson KO, Eccles TK, Lontie R (1981) J Am Chem Soc 103:984–986
13. Co MS, Hodgson KO (1981) J Am Chem Soc 103:3200–3201
14. Woolery GL, Powers L, Winkler M, Solomon EI, Spiro TG (1984) J Am Chem Soc 106:86–92
15. Tan G, Kau L-S, Hodgson KO, Solomon EI (1989) Physica B 158:110–111
16. Magnus K, Ton-That H (1992) J Inorg Biochem 47:20
17. Magnus KA, Ton-That H, Carpenter JE (1994) Chem Rev 94:727–735
18. Kitajima N, Fujisawa K, Moro-oka Y, Toriumi K (1989) J Am Chem Soc 111:8975–8976
19. Eickman NC, Himmelwright RS, Solomon EI (1979) Proc Natl Acad Sci USA 76:2094–2098
20. Himmelwright RS, Eickman NC, LuBien CD, Lerch K, Solomon EI (1980) J Am Chem Soc 102:7339–7344
21. Prota G (1988) Med Res 8:525–556
22. Mason HS (1956) Nature 177:79–81
23. Jolley RL Jr, Evans LH, Mason HS (1972) Biochem Biophys Res Commun 46:878–884
24. Jolley RL Jr, Evans LH, Makino N, Mason HS (1974) J Biol Chem 249:335–345
25. Woolery GL, Powers L, Winkler M, Solomon EI, Lerch K, Spiro TG (1984) Biochim Biophys Acta 78:155–161
26. Kertesz D, Rotilio G, Brunori M, Zito R, Antonini E (1972) Biochem Biophys Res Commun 49:1208–1215
27. Eickman NC, Solomon EI, Larrabee JA, Spiro TG, Lerch K (1978) J Am Chem Soc 100:6529–6531
28. Trémolière M, Bieth JB (1984) Phytochemistry 23:501–505
29. Fischer H (1991) PhD Thesis, University of Münster
30. Bradford MM (1976) Anal Biochem 72:248–254
31. Hillenkamp F, Karas M, Beavis RC, Chait BT (1991) Anal Chem 63:1193A–1203A
32. Hillenkamp F, Karas M (1990) Methods Enzymol 193:280–295
33. Forsyth WGC, Quesnel VC (1957) Biochim Biophys Acta 25:155–160
34. Forsyth WCG, Quesnel VC, Roberts JB (1960) Biochim Biophys Acta 37:322–326
35. Nahrstedt A, Albrecht M, Wray K, Gumbinger HG, John M, Winterhoff H, Kemper FH (1990) Planta Med 56:395–398
36. Cilliers JJL, Singleton VL (1991) J Agric Food Chem 39:1298–1303
37. Keilin D, Mann T (1938) Proc R Soc Lond B 125:187–204
38. Chakraborty AK, Orlow SJ, Pawelek JM (1992) FEBS Lett 302:126–128
39. Himmelwright RS, Eickman NC, Solomon EI (1979) Biochem Biophys Res Commun 86:628–634
40. Himmelwright RS, Eickman NC, LuBien CD, Solomon EI (1980) J Am Chem Soc 102:5378–5388
41. Wilcox DE, Long JR, Solomon EI (1984) J Am Chem Soc 106:2186–2194
42. Broman L, Malmström BG, Aasa R, Vänngård T (1962) J Mol Biol 5:301–310
43. Krebs B (1995) In: Kessissoglou DP (ed) Bioinorganic Chemistry: An Inorganic Perspective of Life. Kluwer, Dordrecht, pp 371–384
44. Ghiretti F (1956) Arch Biochem Biophys 63:165–176
45. Ling J, Nestor LP, Czernuszewicz RS, Spiro TG, Fraczkiewicz R, Sharma KD, Loehr TM, Sanders-Loehr J (1994) J Am Chem Soc 116:7682–7691
46. Baldwin MJ, Root DE, Pate JE, Fujisawa K, Kitajima N, Solomon EI (1992) J Am Chem Soc 114:10421–10431
47. Kitajima N, Fujisawa K, Fujimoto C, Moro-oka Y, Hashimoto S, Kitagawa T, Toriumi K, Tatsumi K, Nakamura A (1992) J Am Chem Soc 114:1277–1291
48. Karlin KD, Hayes JC, Gultneh Y, Cruse RW, McKown JW, Hutchinson JP, Zubieta J (1984) J Am Chem Soc 106:2121–2128
49. Rompel A, Fischer H, Büldt-Karentzopoulos K, Meiwes D, Zippel F, Nolting HF, Hermes C, Krebs B, Witzel H (1995) J Inorg Biochem 59:715
50. Kitajima N, Moro-oka Y (1994) Chem Rev 94:737–757